1990A&A...230..463J

Astron. Astrophys. 230, 463–473 (1990)

ASTRONOMY AND ASTROPHYSICS

Can stellar dynamos be modelled in less than three dimensions?

R. Jennings[1], **A. Brandenburg**[2], **D. Moss**[2,3], **and I. Tuominen**[2]

[1] Department of Mathematics and Statistics, The University, Newcastle Upon Tyne NE1 7RU, UK
[2] Observatory and Astrophysics Laboratory, University of Helsinki, Tähtitorninmäki, SF-00130 Helsinki, Finland
[3] Department of Mathematics, The University, Manchester M13 9PL, UK

Received August 2, accepted August 25, 1989

Abstract. Direct comparisons are made between nonlinear $\alpha\omega$-dynamos in different geometries. We investigate the importance of radial structure by comparing results of axisymmetric 1-D models with their 2-D counterparts. These 2-D models can either be fully spherical or in a shell resembling a stellar convection zone. The importance of treating the curvature associated with the polar regions is also considered by comparing results in Cartesian coordinates with those in spherical geometry. It turns out that omitting curvature in a model has only minor effects on the magnetic fields and on details of bifurcations for mixed parity solutions. In contrast dropping the radial extension leads to quite different bifurcation diagrams. However gross features like the transition between two opposite parities via a mixed parity solution occur in the bifurcation diagram for both cases. A more subtle effect is that finite amplitude solutions stable to axisymmetric perturbations can lose their stability when subjected to the more general non-axisymmetric perturbations. From this we conclude that the stability properties of a stellar dynamo can only be determined with certainty once fully 3-D perturbations have been considered. For the 2-D non-axisymmetric extension of the 1-D model we find a finite amplitude mixed solution with non-axisymmetric contributions. Finally we show that previously investigated mixed parity torus-type solutions in spherical geometry are stable against 3-D perturbations.

Key words: Sun: magnetic fields – mean-field dynamo – stability – non-axisymmetric magnetic fields

1. Introduction

Many physical phenomena can be understood in terms of simplified (truncated) models. For example insight can be gained about the dynamics of a complicated system using a low order model. The classic example is the Lorenz system of equations associated with weather prediction (Lorenz, 1963) which clearly demonstrated many nonlinear phenomena previously not well understood, including the so-called strange attractor. Other low order models have successfully reproduced the aperiodic time series typical of the solar cycle (Weiss et al., 1984). In that model the differential rotation was coupled dynamically to the field, as is thought to be the case for the torsional oscillations observed by Howard and LaBonte (1980). Clearly there are dangers associated with truncated systems, and results should be interpreted cautiously. Recent studies of a truncated 1-D $\alpha\omega$-dynamo model by Jennings and Weiss (1990a, b) have provided some new insight to the detailed bifurcation phenomena in the far nonlinear regime. They were able to explore the parameter space up to very large dynamo numbers, which was possible due to the reduced computational effort required for low order systems together with the feasibility of performing detailed analysis on nonlinear solutions. They employed a numerical procedure which could find both unstable and stable solutions. By using Floquet theory to determine the stability of periodic solutions, it was then possible to construct the full bifurcation diagram.

Such results are qualitatively useful for showing the possible finite amplitude states of a supercritical stellar dynamo. However, having neglected curvature and radial structure it is important to compare the results with more realistic models in spherical geometry. For example the bifurcation and stability properties of spherical axisymmetric models found by Brandenburg et al. (1989a, b) seem to be qualitatively similar to those by Jennings and Weiss.

The early $\alpha\omega$-dynamos by Steenbeck and Krause (1969) are of pure parity, associated with the perfect symmetries imposed by the α and ω-effect. The magnetic field configuration can either be symmetric (S) or antisymmetric (A) about the equatorial plane. However, the more recent studies mentioned above find the pure solution can lose stability to a solution of "mixed parity" as the dynamo number is increased. For even higher dynamo numbers the results are model dependent, and the mixed parity solution can either lose stability to another pure solution or to another mixed solution. Thus there is some qualitative agreement between the 1-D and 2-D models whilst there are also differences. These differences will be discussed in more detail in later sections.

From the observational point of view one is mainly interested in the magnetic field in the surface layers of a star. In the case of axisymmetric field configurations one usually compares observations and the model in terms of butterfly diagrams ($\theta-t$-maps). The Jennings and Weiss paper which has only θ and t dependence was formulated with this in mind. For non-axisymmetric fields one can employ surface maps (via surface imaging, e.g. Piskunov et al., 1990). It is therefore tempting to directly compute such "observational maps" rather than deriving them from full 3-D simulations. This idea is central to the approximation of mean-field electrodynamics, where only the mean field is computed, and nothing is learnt about the small scale fluctuating magnetic field.

Send offprint requests to: R. Jennings

© European Southern Observatory • Provided by the NASA Astrophysics Data System

1990A&A...230..463J

It has been stressed recently by Krause and Meinel (1988) that the stability of nonlinear solutions of the dynamo equations are of basic importance to explanations of cosmical magnetic fields. They showed for a simple 1-dimensional model that only the solution with the smallest critical dynamo number can be stable, with all other solutions bifurcating from the trivial solution initially unstable. However, this result only applies to a neighbourhood of the marginal value of the excitation parameters and we cannot make general deductions about stability using linear analysis of the trivial solution and weakly nonlinear theory alone. Moreover, Rädler and Wiedemann (1989) have demonstrated for an α^2-dynamo model that stability analysis restricted to 2-D disturbances can lead to the wrong conclusions. For example, at certain parameter values S0 and A0 type solutions are stable to axisymmetric disturbances, but only the A0 solution is stable when non-axisymmetric disturbances are considered (Sm and Am denote solutions symmetric and antisymmetric about the equator, where m is the spherical harmonic order).

The possibility of non-axisymmetric solutions, or at least non-axisymmetric contributions to mixed solutions, should also be considered for models in which the radial dimension is omitted. On the other hand, the radial extension of the fields may be very important for the field topology of non-axisymmetric configurations. Models with full radial dependence are particularly hard to treat numerically in the case of $\alpha\omega$-dynamos because very short time steps are needed to resolve the strong winding-up of field lines (Rädler, 1986b; Rädler et al., 1990). Such difficulties cannot arise in a model without radial structure, which has the advantage of making the analysis easier, but the associated disadvantage that the important effect of winding up of field lines is ignored.

From linear theory we know that the marginal dynamo numbers of non-axisymmetric field modes are considerably higher than for axisymmetric modes when differential rotation is important. Therefore the existence of secondary bifurcations to solutions with non-axisymmetric contributions seems the most plausible explanation of non-axisymmetric fields in systems with strong differential rotation. This may be important in understanding the active longitudes on the Sun (e.g. Bai, 1988) or non-axisymmetric fields on stars.

The paper is arranged as follows. In Sect. 2 we present the basic equations and definitions associated with axisymmetric $\alpha\omega$-dynamos and we compare the results of various axisymmetric models in different geometries. From these results we can deduce the consequences of neglecting either or both radial structure and curvature. A new non-axisymmetric model is derived in Sect. 3 which is still 2-D because the radial structure is omitted. Linear and nonlinear results for this model are presented. In the following section we then determine the linear 3-D stability properties of nonlinear axisymmetric solutions for a spherical model. Finally, in the last section we present some conclusions.

2. The axisymmetric $\alpha\omega$-dynamo

The generation of magnetic fields can be described by the standard induction equation for the mean field,

$$(\partial_t - \nabla^2)\boldsymbol{B} = \mathrm{curl}(\alpha\boldsymbol{B} + \boldsymbol{u}\times\boldsymbol{B}), \tag{1}$$

together with

$$\nabla\cdot\boldsymbol{B} = 0, \tag{2}$$

where $\alpha = \tilde{\alpha}\cos\theta$ parameterizes the effect of cyclonic convection on the mean magnetic field, $\boldsymbol{B}$. The macroscopic velocity field consists only of the rotational velocity $\boldsymbol{u} = \hat{\boldsymbol{\phi}}\Omega r\sin\theta$, where Ω is the angular velocity. We use dimensionless units, measuring length in units of the stellar radius, R, and time in units of R^2/η, where η is a turbulent magnetic diffusivity which is assumed to be constant. The quantities $\boldsymbol{u}$, $\boldsymbol{B}$, and α should be coupled via a momentum equation. For convenience we by-pass this coupling by including idealised nonlinear terms in the induction equation. In this section we assume an α-quenching mechanism with $\tilde{\alpha} = \alpha_0/(1+|\boldsymbol{B}|^2)$. Restricting our attention to purely axisymmetric fields ($\partial_\phi = 0$) in a spherical coordinate system (r, θ, ϕ) allows $\boldsymbol{B}$ to be represented in the form:

$$\boldsymbol{B} = b\hat{\boldsymbol{\phi}} + \mathrm{curl}(a\hat{\boldsymbol{\phi}}), \tag{3}$$

which leads to the following equations for the scalars a and b:

$$\begin{aligned}(\partial_t - \mathrm{D}^2)a &= \alpha b\\ (\partial_t - \mathrm{D}^2)b &= \Omega'\partial_\theta(\sin\theta\, a) + \ldots,\end{aligned} \tag{4}$$

where $\Omega' = \partial\Omega/\partial r$, and Ω is the angular velocity which is assumed to depend only on r. The operator D^2 is defined by

$$\mathrm{D}^2 a \equiv -\hat{\phi}\cdot\mathrm{curl}\,\mathrm{curl}\,(a\hat{\phi}) = \frac{1}{r}\frac{\partial^2}{\partial r^2}(ra) + \frac{1}{r^2}\frac{\partial}{\partial\theta}\left[\frac{1}{\sin\theta}\frac{\partial}{\partial\theta}(\sin\theta\, a)\right]. \tag{5}$$

The relative magnitudes of the α and ω-effects are measured by the numbers $C_\alpha = \alpha_0$ and $C_\omega = \partial\Omega/\partial r$. The dots in Eq. (4) indicate the existence of an additional α-effect for the generation of b from a, which is neglected in several cases considered below (pure $\alpha\omega$-dynamo). This corresponds to the limit $C_\alpha/C_\omega \ll 1$, which is often applied in stellar dynamo theory. Some of the models described in later sections have taken the full α-effect into account, and we speak then of an $\alpha^2\omega$-dynamo. The important control parameter is the dynamo number $D = C_\alpha C_\omega$ (not to be confused with the operator D^2). In comparison with the solar field we note that for $D<0$ we obtain the "correct butterfly diagram", i.e. dynamo waves migrating towards the equator.

2.1. *The importance of radial structure*

At first it may seem crucial to have detailed radial structure in a dynamo model with differential rotation. Nevertheless, if the angular velocity is prescribed and the velocity field is not calculated explicitly from the momentum equation, radial derivatives only appear in the diffusion operator of the pure $\alpha\omega$-dynamo equations (4). Thus in the 1-D approximation we are essentially simplifying the diffusion term.

For dynamos in thin shells radial diffusion will eventually dominate over latitudinal diffusion, and 1-D models fail to reflect this, even though it is tempting to associate such models with the limit of thin layers. Averaging the equations formally over the layer introduces "jump" conditions which depend upon the radial boundary conditions (Greenspan, 1974). For certain radial boundary conditions however, these "jumps" are all zero, leading to fields independent of radial structure as used by Jennings and Weiss.

The new feature in the flat (no curvature) 1-D dynamo of Jennings and Weiss, that for slightly supercritical negative dynamo numbers a steady quadrupolar mode (S0) is excited first, is similar to the behaviour found by Stix (1975) for flat galactic

© European Southern Observatory • Provided by the NASA Astrophysics Data System

1990A&A...230..463J

dynamos, in which a branch of steady S0 modes acquired a positive growth rate at low D. This linear growth rate continued to grow before reaching a maximum and subsequently became negative at a larger value of D. Such linear theory can be very misleading though when it comes to finite amplitude solutions, since for α-quenching in the Jennings and Weiss model this S0 mode did not destabilise (see Fig. 1a) with increasing D, as it did in cases with other nonlinearities. This shows all too clearly the dangers of drawing conclusions based on linear theory alone.

Another property of 1-D models, which is not typical of 2-D models, is that the marginal dynamo numbers for different modes are very far apart. Also the energies belonging to solutions with opposite parity can be quite different (see Fig. 1 and Table 1). This is similar to the result for another 1-D α^2-dynamo model (no ω-effect) in a slab, where α changes sign in the middle of the layer (see Fig. 6a in Brandenburg et al., 1989a). In contrast, the energies for 2-D dynamos with the same α-quenching are closer together (cf. Brandenburg et al., 1989b, 1990).

In the 1-D approximation the nonlinearity due to buoyancy causes a very rich bifurcation diagram. Typically two branches belonging to solutions with opposite parity are connected by a mixed-mode branch. This was found also in the 2-D dynamo in a sphere, but only for α-quenching and not when buoyancy effects become dominant (Moss et al., 1990).

We may summarize that neglecting the radial extension of the dynamo region leads to quite marked changes in the bifurcation diagrams. However there are also features, such as the transition between two opposite parities via a mixed parity solution, which occur in the bifurcation diagram for both cases.

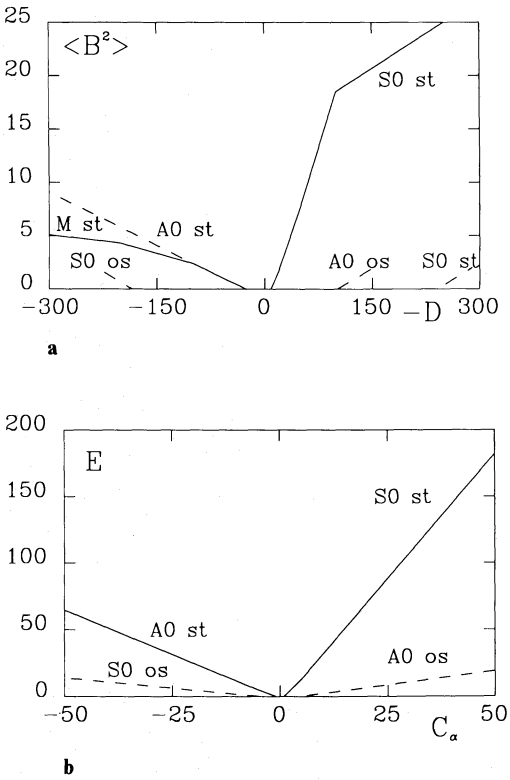

Fig. 1a and b. Bifurcation diagram for a 1-D dynamo model without radial extension **a** without curvature and **b** with curvature. Stationary solutions are denoted by "st" and oscillatory ones by "os"

2.2. *Comparison with shell dynamos*

Another way to investigate the influence of radial structure is to treat a spherical shell, in which the parameter varied is the shell thickness. In the following we shall compare the 1-D models with results obtained for such "shell dynamos".

We reduce the computational domain to $0.7<r<1$, assuming a perfect conductor boundary condition at a radius $r=0.7$ (Köhler, 1973). It turns out that the marginal dynamo numbers for symmetric and antisymmetric fields are very close together. Also torus-type mixed parity solutions are still possible. However, the winding numbers (or ratios between the two periods) are typically much higher than for dynamos operating in the entire sphere. (More details are given in Brandenburg et al., 1990.)

It seems that the step from the sphere to a shell takes us further away from the Jennings and Weiss type model. This confirms the suggestion that for dynamos in a thin shell radial diffusion is important, that is the 1-D model does *not* correspond to the limit of thin shells.

The solar dynamo is probably located at the bottom of the convection zone (Parker, 1979; see also Schüssler, 1983). In contrast to a shell dynamo with constant α-distribution and a vacuum boundary condition at the top of the layer we are now left with a thick diffusion region on top of the α-layer. This diffusion layer may smooth out the radial gradients and probably better resembles the 1-D approximation by Jennings and Weiss. In order to check this we computed a model with an α-effect confined to the bottom of the convection zone at $r=0.7$. The profile adopted for α corresponds to that given by Rädler (1986a, Eq. (13)) which has a maximum at $r=0.7$ and a width of $d=0.1$.

Table 1. Steady solutions with α-quenching (Jennings and Weiss, 1989b). The letters s, u, and m refer to stable, unstable and marginal stability

	S0		A0	A0+S0
D	$\langle B^2\rangle$	D	$\langle B^2\rangle$	$\langle B^2\rangle$
−20	1.71 s	35	0.27 s	—
−50	7.74 s	55	0.91 s	—
−100	18.46 s	84	1.90 m	1.90 m
−600	31.77 s	100	2.41 u	2.40 s
−1000	214.1 s	200	5.77 u	4.26 s
−2000	431.6 s	300	9.14 u	5.08 u
−20000	4347 s	1900	63.1 u	21.8 u

We find that a steady S0 solution is now most easily excited, as in Jennings and Weiss. However, the marginal dynamo numbers for A and S type solutions (symmetric and antisymmetric, respectively) are again quite close together and both oscillatory. Thus, a dynamo with a concentration of α at the bottom of the convection zone cannot be simulated by the 1-D model either.

2.3. *The role of curvature in the 1-D dynamo*

We study now a modified 1-D dynamo with curvature simply by dropping the r-derivatives in our code for solving 2-D axisymmetric dynamo equations. The survey is restricted to the case of

© European Southern Observatory • Provided by the NASA Astrophysics Data System

1990A&A...230..463J

Table 2. The logarithm (base ten) of the energies for the axisymmetric model with curvature but no radial structure. For the oscillatory solutions the minimum and maximum values are given. The periods are given in square brackets and $C_\omega = -1000$

lg E [period]			lg E [period]		
C_α	A0	S0	C_α	A0	S0
−1	−0.59 s [0]				
−5	0.69 s [0]	−1.10 ... −0.75 u [0.08]	5	−1.59 ... −0.79 u [0.08]	1.12 s [0]
−50	1.81 s [0]	−0.63 ... 1.14 u [0.075]	50	0.45 ... 1.28 u [0.10]	2.26 s [0]
−500	2.83 s [0]	2.75 u [0]			

α-quenching. The results found are very similar to those of Jennings and Weiss: a steady S0 solution is excited most easily (for $D<0$), and at larger dynamo numbers an oscillatory A0 solution of much smaller amplitude is strongly suppressed by the S0 mode. For $D>0$ the roles of S and A are interchanged, see Fig. 1b, and Table 2.

Testing the stability of finite amplitude solutions by perturbing with a solution of opposite parity (Brandenburg et al., 1989a) we find only the steady solutions to be stable, even at dynamo numbers as large as 5×10^4. This is in slight contrast to stability behaviour of the solutions of Jennings and Weiss, where the stationary A0 solution becomes unstable to a stationary mixed solution (S0+A0) at large (and positive) dynamo numbers (see Fig. 1). This difference can only be attributed to the absence of curvature in the Jennings and Weiss equations.

2.4. The role of curvature in the 2-D dynamo

The effect of curvature can be studied by limiting the computational domain to $\theta_1<\theta<\theta_2$ (with $0<\theta_1,\theta_2<\pi$), that is by cutting off the polar regions. We have done this with our 2-D code by imposing a perfect conductor boundary condition at some intermediate latitudes. An understanding of the consequences of this somewhat arbitrary condition is important, because 3-D codes in spherical geometry based on finite difference methods cannot cope easily with the singularities at the pole. For example, Gilman and Miller (1981) found it necessary to introduce a perfect conductor boundary at 70° latitude. This condition implies that the θ-component of the magnetic field and the r- and ϕ-component of the electric field both vanish at some latitudes $\theta=\theta_1,\theta_2$. In terms of a and b we have, in the presence of an α-effect,

$$\left.\begin{aligned} a&=0\\ \partial_\theta(\sin\theta b)&=\alpha\partial_\theta(\sin\theta a)\end{aligned}\right\}\quad\text{on }\theta=\theta_1,\theta_2. \tag{6}$$

(If α is assumed to vanish at $\theta=\theta_1,\theta_2$ we are then effectively using the conditions of Gilman and Miller.)

Taking the dynamo as being confined in a shell with inner radius $r_0=0.7$ we find, at slightly supercritical dynamo numbers, essentially the same bifurcations in both cases, with and without restricted latitudinal extent. That is, in both cases there is an A0-type solution with dynamo waves migrating to the equator with approximately the same frequency. Both field geometries are displayed in Fig. 2. However, in contrast to the case where the poles are included, the pure A0-solutions no longer lose stability as the dynamo number is increased. This indicates that the torus-type solutions described in Brandenburg et al. (1989b) require the inclusion of the polar regions. On the other hand the basic dynamo cycle is still very similar to the original situation in a full spherical shell. So we may conclude that the sine and cosine terms (curvature) do modify the oscillatory αω-dynamo qualitatively, but the basic dipolar type field configuration found for sufficiently low dynamo numbers is largely unaffected by curvature.

To summarize we can say that omitting curvature in a model has comparatively little influence on the magnetic fields and on the details of bifurcations to mixed solutions compared to the more drastic consequences of omitting the radial extension.

3. A non-axisymmetric dynamo ($\partial_y\neq0$)

The investigations of nonlinear and non-axisymmetric αω-dynamos is still restricted to cases of weak differential rotation. This is mainly because non-axisymmetric fields are wound up very tightly, due to the differential rotation, in such a way that oppositely directed field lines lie very close together (cf. Rädler, 1986a). This introduces very short length-scales which have to be resolved by the model, and the necessity of using very short time steps becomes inevitable. Furthermore, the short length scales in the field structure give rise to an enhanced dissipation, which, according Rädler (1986b), makes non-axisymmetric dynamos very hard to excite in the presence of strong differential rotation. However, this winding-up of field lines is not present in a model without radial extent, and it is therefore not clear, whether such a model could be of relevance for understanding non-axisymmetric αω-dynamos.

In the following we shall consider dynamo action in a thin layer. By making certain simplifications we proceed to derive equations for two scalar potentials (toroidal and poloidal), starting from the induction equation for $\boldsymbol{B}$. Here we choose a different nonlinearity (buoyancy) to the α-quenching discussed earlier. This is because the nonlinear results for α-quenching in the 1-D model are not very interesting, and the extra azimuthal structure seems unlikely to affect the results. Further, the treatment of the coupling between the axisymmetric and non-axisymmetric perturbations is more difficult in the case of α-quenching.

3.1. Model equations

We extend the 1-D models of Jennings and Weiss to include azimuthal or y-dependence. We make certain assumptions which effectively remove all radial dependence from the equations. Rather than model the instability of individual flux tubes due to

© European Southern Observatory • Provided by the NASA Astrophysics Data System

1990A&A...230..463J

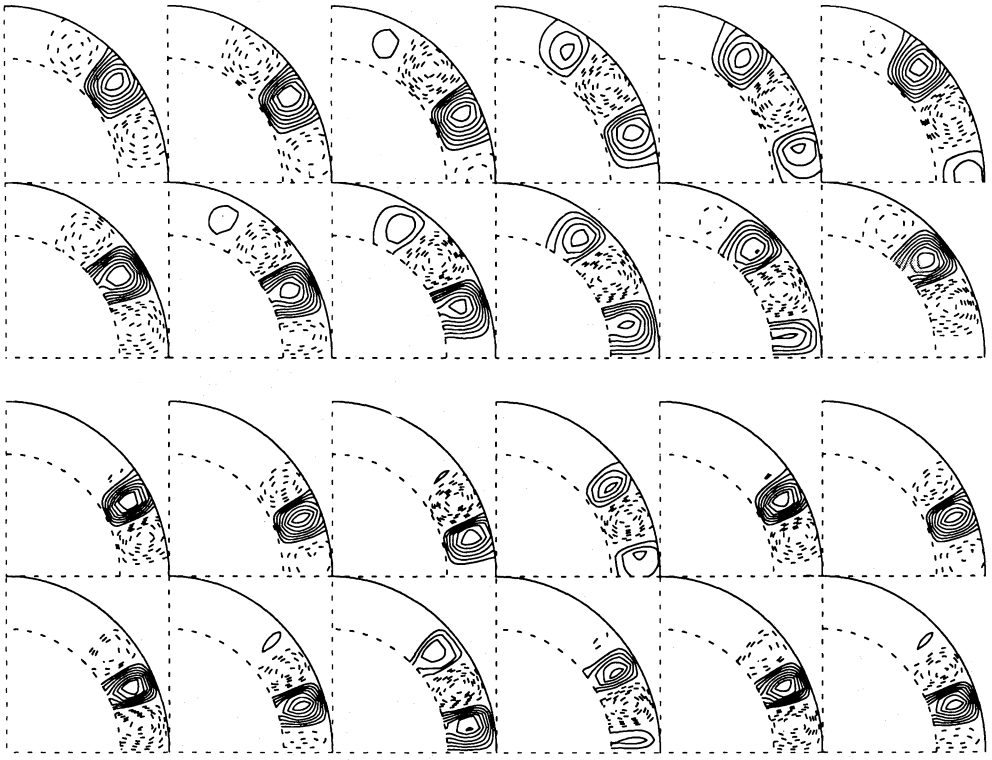

Fig. 2. The effect of curvature demonstrated by an arbitrarily introduced perfect conductor boundary condition at 45° latitude. Snapshots of poloidal field lines and contours of constant toroidal field are plotted for a complete cycle without latitudinal boundaries (upper two rows) and with $\theta_1 = 45°$ (lower two rows). Broken contours denote a negative sign

buoyancy (Hughes, 1985), we simplify in the spirit of the mean-field approximation and assume that such flux losses occur smoothly when averaged over small scales. The induction equation now has an additional nonlinear radial velocity $\boldsymbol{u}_B$ which models toroidal flux loss due to buoyancy:

$$(\partial_t - \nabla^2)\boldsymbol{B} = \mathrm{curl}(\alpha\boldsymbol{B} + \boldsymbol{u}\times\boldsymbol{B} + \boldsymbol{u}_B \times B_y\hat{\boldsymbol{y}}) \tag{7}$$

with $\alpha = C_\alpha \cos x$, $\boldsymbol{u} = C_\omega z \sin x \hat{\boldsymbol{y}}$. Cartesian coordinates (x, y, z) correspond to spherical polar coordinates (θ, ϕ, r) respectively, with $0 \le x \le \pi$, $0 \le y \le 2\pi$, and z extends across a "thin" layer. The velocity $\boldsymbol{u}_B$ depends only on the azimuthal field B_y, since this is the dominant field in $\alpha\omega$-dynamos. In order that the nonlinear velocity $\boldsymbol{u}_B$ is independent of the sign of B_y, we assume $\boldsymbol{u}_B$ proportional to B_y^2. In this simple form it is the radial gradient $\partial_r \boldsymbol{u}_B$ which is most important, and in the same spirit as adopted for the azimuthal velocity we take a linear profile in z: $\boldsymbol{u}_B = \lambda z B_y^2 \hat{\boldsymbol{z}}$, with $\lambda = \mathrm{const}$.

Within the thin layers we assume $\boldsymbol{B}$ to be independent of height z, and therefore we do not need to specify any radial boundary conditions for $\boldsymbol{B}$ at the top and bottom of the layer. The velocities $\boldsymbol{u}$ and $\boldsymbol{u}_B$ have an idealised z structure such that ∂_z is constant. Since we are only solving for $\boldsymbol{B}$ independent of z we can treat the induction equation at any height ($z = \mathrm{const}$), and we choose $z = 0$ without loss of generality. Essentially we have adopted the following spatial scaling for $\boldsymbol{B}$: $\partial_z \ll \partial_x, \partial_y$, with ∂_x, ∂_y both $O(1)$.

Since $\boldsymbol{B}$ is divergence free it is natural to express $\boldsymbol{B}$ in terms of toroidal and poloidal functions

$$\boldsymbol{B} = \mathrm{curl}\,\mathrm{curl}(\hat{\boldsymbol{z}}\phi) + \mathrm{curl}(\hat{\boldsymbol{z}}\psi). \tag{8}$$

Substituting Eq. (8) into (7), and making appropriate scalings to ϕ and ψ, together with the limit $C_\alpha \ll C_\omega$, gives:

$$\mathscr{D}\Phi = D\nabla_H \cdot (\cos x \nabla_H \psi),$$
$$\mathscr{D}\Psi = \partial_x(\sin x \Phi) - \partial_x[(\partial_x\psi)^3], \tag{9}$$

where $\mathscr{D} \equiv (\partial_t - \nabla_H^2)$, and $\nabla_H \equiv (\partial_x, \partial_y, 0)$. Variables Φ and Ψ are related to ϕ and ψ by Poisson type equations:

$$\nabla_H^2 \phi = \Phi,$$
$$\nabla_H^2 \psi = \Psi, \tag{10}$$

where the z independent $\boldsymbol{B}$ is given explicitly by

$$\boldsymbol{B} = (\partial_y\psi, -\partial_x\psi, -\Phi). \tag{11}$$

3.2. *The boundary conditions*

Periodic boundary conditions are used for $\boldsymbol{B}$ in the y-direction, but the conditions at the poles are not so obvious in this geometry. In a sphere, the $\theta - \phi$-dependence of the potentials in Eq. (8) can be expanded in terms of spherical harmonics $P_n^m(\cos\theta)$, if the external magnetic fields are taken to be current free (Stix, 1971). We assume that ϕ, ψ have the same behaviour at the poles as $P_n^m(\cos\theta)$, that is:

$$\phi = \psi = 0 \quad \text{at} \quad x = 0, \pi \quad \text{if} \quad m \neq 0,$$
$$\partial_x\phi = \partial_x\psi = 0 \quad \text{at} \quad x = 0, \pi \quad \text{if} \quad m = 0. \tag{12}$$

Note that such conditions in this geometry make the θ-component of field vanish at the poles. This is unphysical, but arises because we have neglected the $(\sin x)^{-1}$ factor associated with the curvature in $B_\theta = (\sin x)^{-1}\partial_y\psi$ in spherical geometry. However, we are still solving for the correct form of potential ψ and the actual value of B_θ does not directly affect the results.

© European Southern Observatory • Provided by the NASA Astrophysics Data System

1990A&A...230..463J

3.3. *Axisymmetric solutions* ($\partial_y = 0$)

Uncurling Eq. (9) once recovers the system studied by Jennings and Weiss (1989b):

$$\mathscr{D}_x A = D \cos x B_y,$$
$$\mathscr{D}_x B_y = \sin x \partial_x A - B_y^3, \tag{13}$$

where $\mathscr{D}_x$ is the usual 1-D diffusion operator, and $A = -\partial_x \phi$.

3.4. *Non-axisymmetric solutions*

We seek solutions representing travelling waves in the azimuthal direction which can be further classified according to their parity S or A. For non-axisymmetric fields the real part of the following series expansions for the potentials ensure that the boundary conditions are satisfied

$$\phi(x, y, t) = \mathrm{Re}\left[e^{imy} \sum_{n=1}^{\infty} \phi_{nm}(t) \sin nx \right],$$
$$\psi(x, y, t) = \mathrm{Re}\left[e^{imy} \sum_{n=1}^{\infty} \psi_{nm}(t) \sin nx \right]. \tag{14}$$

For practical calculations these series must be truncated, and in all the following analysis (for a single wavenumber m) we truncate each series at $n = 16$. This truncation appeared satisfactory when compared to results with 32 terms for typical parameters.

3.5. *Marginal dynamo numbers*

The system Eq. (9) can be made linear in ϕ and ψ simply by removing the cubic term associated with buoyancy. In a linear analysis of Eq. (9) the time dependence of the coefficients ϕ_n, and ψ_n can be explicitly written as $e^{\sigma t}$, and for each mode we calculate the value of D (positive and negative) for which the real part of σ is zero. If, at these marginal dynamo numbers, σ has a non-zero imaginary part then the field is overstable and oscillates.

Marginal values of D and their corresponding frequencies are given in Table 3. It is seen that axisymmetric modes are the most unstable for $D < 0$, and whether or not non-axisymmetric fields are important depends upon the stability of finite amplitude solutions to non-axisymmetric perturbations, while it is also possible that a pure *Sm* or A*m* type solution could stabilise at large D. For $D > 0$ however, the most unstable mode is S1, meaning that, initially at least, stable nonlinear solutions will be non-axisymmetric (see Fig. 4).

3.6. *Stability of nonlinear axisymmetric solutions*

Before discussing fully the 2-D nonlinear calculations we first examine the stability of the Jennings and Weiss solutions to non-axisymmetric perturbations. Thus we write

$$\phi = \phi_0(x, t) + \varepsilon \phi_1(x, y, t),$$
$$\psi = \psi_0(x, t) + \varepsilon \psi_1(x, y, t), \tag{15}$$

where $\varepsilon \ll 1$, and all terms of $O(\varepsilon^2)$ are neglected. At $O(1)$ the Jennings and Weiss system is recovered while after rescaling, we get at $O(\varepsilon)$:

$$\mathscr{D}\Phi_1 = D \nabla_H \cdot (\cos x \nabla_H \psi_1),$$
$$\mathscr{D}\Psi_1 = \partial_x(\sin x \Phi_1) - \partial_x(B_y^2 \partial_x \psi_1). \tag{16}$$

Table 3. Marginal dynamo numbers and frequencies for the (non-axisymmetric) 2-D model without radial extent

Mode	D	Frequency	D	Frequency
A0	−102	4.56	26	0
A1	−803	28.31	108	3.00
A2	−1231	34.42	305	7.17
S0	−9	0	189	9.36
S1	−429	18.60	15	0
S2	−994	28.29	246	3.00

The axisymmetric solutions are coupled to the perturbations through the nonlinear buoyancy term. The evolution of these small perturbations is followed by stepping the ϕ_n and ψ_n coefficients of Eq. (16) forward in time and using data from the Jennings and Weiss solutions for B_y^2. Non-axisymmetric perturbations of both parities (S1 and A1, for $m = 1$) are considered because either can be coupled to an A0 or S0 solution through the nonlinearity. Yet, since they are linear, the perturbations of each parity do not couple with one another. If the perturbations grow or decay then we say that the purely axisymmetric field is unstable or stable, respectively.

3.7. *Results from the stability analysis*

Stability results are most easily presented on a bifurcation diagram. In Fig. 6, the axisymmetric S0 and A0 solutions of Jennings and Weiss are plotted as solid lines, if stable to 3-D perturbations, and dotted, if unstable. The bifurcations of the axisymmetric and the first non-axisymmetric modes from the trivial solution are summarized in Table 3.

As expected, for positive D the S1 perturbations are unstable from the onset. The steady A0 branch shows no sign of stabilising with increasing D: on the contrary oscillatory A1 perturbations also grow from the pure A0 solution for D larger than 200. Such linear analysis is unable to determine whether or not mixed parity solutions such as S1 + A0 bifurcate from the initially stable pure S1 and D is increased.

The results for negative D are perhaps the most significant for stellar dynamos. The pure A0 branch, which was stable to axisymmetric perturbations, loses stability to a mixed mode consisting of A0 + S1 modes at $D \approx -555$ (see Fig. 3). See Fig. 5b for the resulting S1 field configuration. Note that the field geometry is very similar when the perturbation is applied to the trivial solution, see Fig. 5a. The pure S1 disturbances are oscillatory with a frequency roughly double that of the periodic A0 field at the bifurcation. Increasing D only increases the growth rates of the S1 disturbances, and eventually the A1 disturbances were also excited. From these results we can also draw a *speculative* bifurcation diagram for the non-axisymmetric solutions to the fully nonlinear 2-D equations, see Fig. 6.

3.8. *Fully nonlinear solutions of the model equations*

In order to proceed beyond the linear stability analysis we now solve the fully nonlinear model equations (9) using a finite difference method. ψ is determined at each time step by solving Eq. (10) for Ψ using a successive over-relaxation method. The

© European Southern Observatory • Provided by the NASA Astrophysics Data System

1990A&A...230..463J

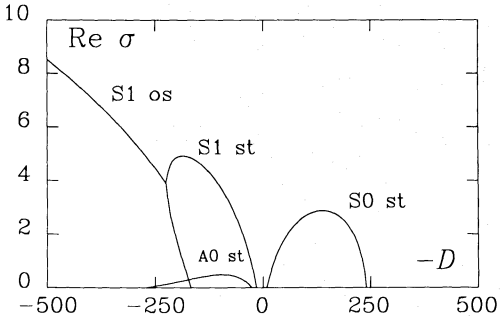

Fig. 3. The growth rates far axisymmetric and non-axisymmetric modes for the 2-D model without radial extent

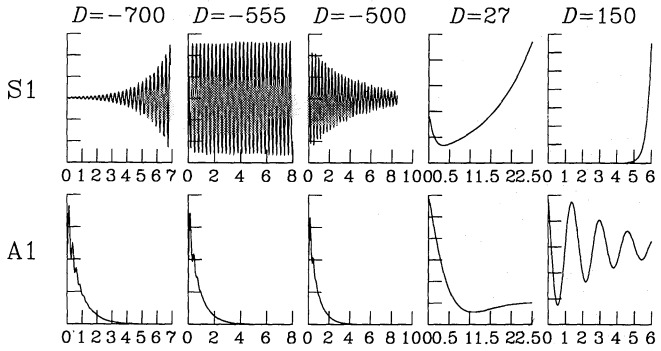

Fig. 4. Stability for S1 and A1 modes for positive and negative dynamo numbers. For $-D<-555$ symmetric perturbations to an axisymmetric field decay, but grow once $-D>-555$. For each dynamo number the antisymmetric perturbations A1 decay to zero. Note that this decay can be either steady or oscillatory. The symmetric perturbations grow steadily for $D>0$

boundary conditions in the form of Eq. (12) cannot be employed in this case, because we need a single condition for solutions containing both axisymmetric and non-axisymmetric fields. We take a condition that mimics the behaviour at the poles in real spherical geometry by introducing a virtual "dummy layer" at $x=-\Delta x$ and $x=\pi+\Delta x$. In this layer the fields are identical with the fields inside the boundary at $x=+\Delta x$ and $x=\pi-\Delta x$ respectively, but shifted in the y-direction by π:

$$\left.\begin{aligned}\Phi(t, x+\Delta x, y)&=\Phi(t, x-\Delta x, y+\pi)\\ \Psi(t, x+\Delta x, y)&=\Psi(t, x-\Delta x, y+\pi)\end{aligned}\right\} \quad \text{on } x=0, \pi. \tag{17}$$

We display the field evolution by means of a parity parameter

$$P=[E^{(S)}-E^{(A)}]/[E^{(S)}+E^{(A)}] \tag{18}$$

and degree of non-axisymmetry by the quantity

$$M=1-E^{(0)}/E, \tag{19}$$

where $E^{(S)}$ and $E^{(A)}$ are the energies contained in the symmetric (S) and antisymmetric (A) part of the magnetic field and $E=E^{(S)}+E^{(A)}$ is the total energy of the magnetic field. $E^{(0)}$ is the energy of the magnetic field averaged over the y-direction.

In Fig. 7 we show the evolution of the quantities E, P, and M for $D=-400$. The initial field configuration was a weak seed field with $P\approx 1$ and $M\approx 1$, that is the field geometry was like that of an S1 mode. Eventually A0 contributions grow leading to a decrease

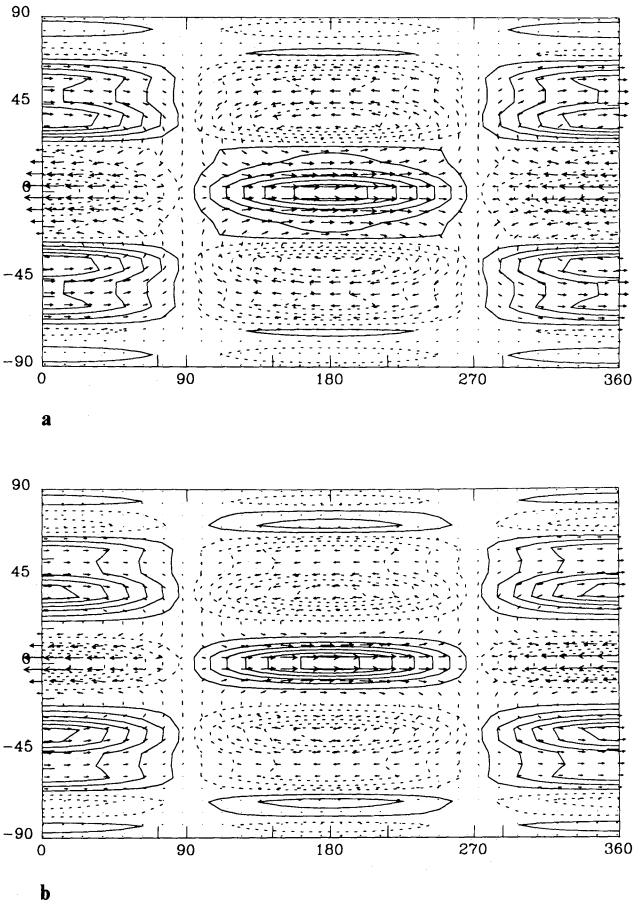

Fig. 5a and b. Non-axisymmetric S1 perturbations from the zero solution at $D=-429$ (**a**) and from a nonlinear A0 solution at $D=-555$ (**b**). The B_x and B_y components are displayed as vectors. Lines of constant B_z are superimposed. Broken contours denote negative values. Note the similarity between the two field configurations

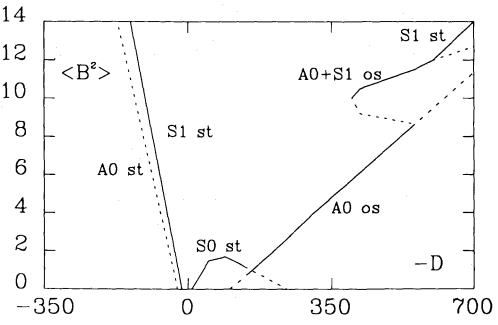

Fig. 6. Bifurcation diagram for the non-axisymmetric dynamo without radial extent. Note the secondary bifurcation from the A0 solution at $D=-555$, leading to a mixed solution consisting of A0 and S1. The branch belonging to this mixed solution is drawn only approximately and is possibly subcritical

of P and M. The final state is a non-axisymmetric periodic mixed parity solution. Snapshots showing the field geometry in three intermediate stages are given in Fig. 8. Since there is no evidence of quasiperiodicity (see Fig. 7) it seems likely that the mixed parity solution has bifurcated from the oscillatory A0 branch

© European Southern Observatory • Provided by the NASA Astrophysics Data System

1990A&A...230..463J

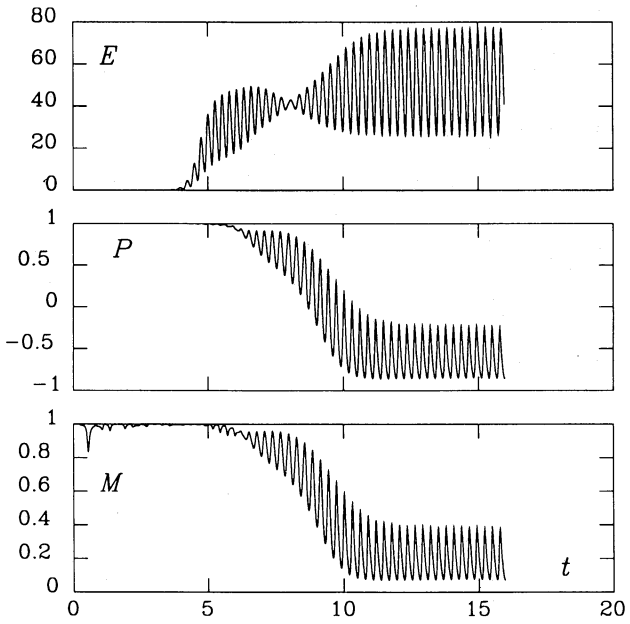

Fig. 7. Nonlinear evolution of E, P, and M for $D=-400$. The final state is a periodically oscillating mixed parity solution

through a pitchfork bifurcation. In the last picture two equatorial field belts with a positive and negative enhancement at two different latitudes can be clearly seen.

The fact that this mixed solution is present at $D=-400$ suggests that the bifurcation at $D=-555$ is subcritical. The mixed solution is therefore initially unstable and only gains stability at a saddle node bifurcation at some $-D>-400$. For $D=-600$ a pure S1 type solution was found showing that a further bifurcation has occurred (for the definition of pure solutions in the non-axisymmetric case see Rädler et al., 1990).

These mixed solutions were obtained using a resolution of 30×31 mesh points, which is probably inadequate to make definitive statements for such highly supercritical dynamo numbers. The computational resources needed are already relatively high, because a very short time step is needed. Thus, and also in view of the approximations of this model which are not physically well motivated (e.g. no radial extend, no winding-up of field lines), we feel that it is not worthwhile to pursue further details of this particular nonlinear model.

4. 3-D stability analysis for a spherical model

Let us now return to the linear stability analysis of non-axisymmetric perturbations of axisymmetric finite amplitude solutions, including full radial structure. The torus-type solutions of the $\alpha\omega$-dynamo equations obtained in fully spherical geometry (Brandenburg et al., 1989b) may just be an artifact of the 2-D approximation employed. We cannot exclude the possibility that the torus solutions are unstable to fully 3-D non-axisymmetric perturbations, similarly to some of the 1-D axisymmetric solutions of Jennings and Weiss (see previous section). This possibility was first demonstrated by Rädler and Wiedemann (1989) for a 3-D α^2-dynamo, where certain nonlinear pure mode solutions were found to be unstable.

4.1. The basic equations

Consider a nonlinear, strictly axisymmetric solution to the mean-field dynamo equation

$$(\partial_t-\nabla^2)\boldsymbol{B}=\mathrm{curl}(\alpha\boldsymbol{B}+\boldsymbol{u}\times\boldsymbol{B}), \tag{20}$$

$\boldsymbol{B}_0(r,\theta,t)$ say. This solution may be time varying or invariant. In principle the nonlinearity can take several plausible forms, but here we focus on the simple "α-quenching" mechanism writing

$$\alpha=C_\alpha\cos\theta/(1+|\boldsymbol{B}_0|^2). \tag{21}$$

The stability of the axisymmetric solution can be tested quite simply by numerically perturbing the solution and following its subsequent time evolution.

4.2. The axisymmetric solutions

Several such α-quenched solutions have previously been described. These displayed a variety of interesting phenomena, such as the coexistence of two stable steady solutions at the same parameter values, and the existence of up to three stable unsteady solutions, including a limit cycle of constant but mixed parity and a torus type solution with large oscillations in the mean parity, and a limit cycle of pure parity (Brandenburg et al., 1989b). The question of the stability of these solutions to non-axisymmetric perturbations naturally arises.

The torus-type solutions mentioned above are obtained for quite strong differential rotation with $C_\omega=-10^4$. In this case the time scale associated with non-axisymmetric solutions are very short. Conveniently we find very similar bifurcation properties when $C_\omega=-10^3$, if C_α is increased by a factor of ten. The basic parameter in this parameter range is therefore the dynamo number D. For example, torus-type solutions were found for $C_\alpha=8.5$ and 9.0. The long term oscillations in E and P are displayed in Fig. 9. Pure A0-solutions are stable for $C_\alpha\lesssim 7.5$ and pure S0-solutions are stable for $C_\alpha\gtrsim 10.0$. For $C_\alpha=8.0$ there is a stable mixed parity limit cycle solution. Properties of these solutions are summarized in Table 4.

4.3. The linearized equations

Write $\boldsymbol{B}(r,\theta,\phi,t)=\boldsymbol{B}_0(r,\theta,t)+\boldsymbol{B}_1(r,\theta,\phi,t)$, where $|\boldsymbol{B}_1|\ll|\boldsymbol{B}_0|$. Substituting into Eq. (20) and linearizing gives

$$(\partial_t-\nabla^2)\boldsymbol{B}_1=\mathrm{curl}(\boldsymbol{u}\times\boldsymbol{B}_1+\alpha_0\boldsymbol{B}_1)+\mathrm{curl}(\alpha_1\boldsymbol{B}_0), \tag{22}$$

where $\alpha_0=\alpha(\boldsymbol{B}_0,\cos\theta)$ and

$$\alpha_1=-2\boldsymbol{B}_0\cdot\boldsymbol{B}_1\alpha_0/(1+|\boldsymbol{B}_0|^2). \tag{23}$$

Eq. (22) is just the linear dynamo equation for $\boldsymbol{B}_1$ with the additional term $\mathrm{curl}(\alpha_1\boldsymbol{B}_0)$. Given the function $\alpha_0(r,\theta,t)$, Eq. (22) can be integrated forward in time for an arbitrary initial perturbation $\boldsymbol{B}_1(t=0)$.

The energy, E, of the non-axisymmetric field contained in the volume of integration eventually will either grow or decay exponentially (if E oscillates, then replace E by its average over a cycle). If E grows, the solution $\boldsymbol{B}_0(r,\theta,t)$ is unstable to small perturbations, otherwise it is stable. The growth rate of the dominant mode is given by $\frac{1}{2}d\ln E/dt$. This approach can, however, say nothing about metastability, nor the long term evolution of an unstable solution. To answer these questions a fully nonlinear code is required.

© European Southern Observatory • Provided by the NASA Astrophysics Data System

1990A&A...230..463J

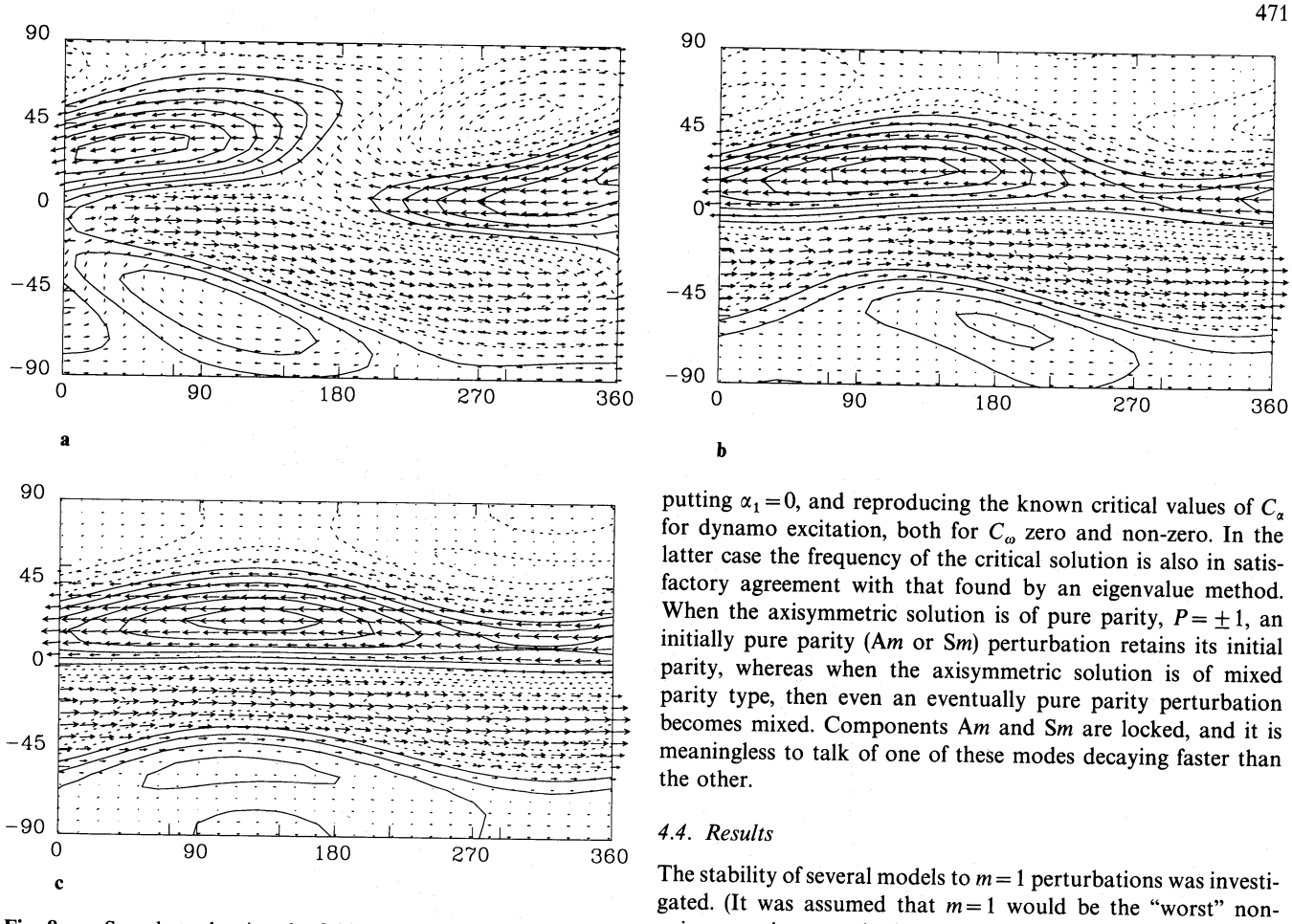

Fig. 8a–c. Snapshots showing the field configuration at times 9.9 (**a**), 10.4 (**b**) and 12.0 (**c**). Vectors and contours have the same meaning as in Fig. 5

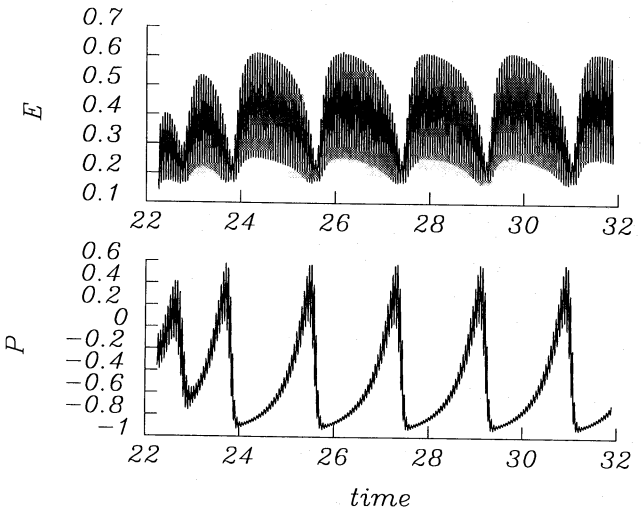

Fig. 9. Long term oscillations in E and P for $C_\alpha = 8.5$ and $C_\omega = -10^3$

A code has been written (in complex arithmetic) to solve Eq. (22) for a single azimuthal Fourier mode m ($\boldsymbol{B}_1 \propto \exp(im\phi)$). The zero order field, $\boldsymbol{B}_0$, is calculated simultaneously by the standard axisymmetric dynamo code. It has been tested by putting $\alpha_1 = 0$, and reproducing the known critical values of C_α for dynamo excitation, both for C_ω zero and non-zero. In the latter case the frequency of the critical solution is also in satisfactory agreement with that found by an eigenvalue method. When the axisymmetric solution is of pure parity, $P = \pm 1$, an initially pure parity (Am or Sm) perturbation retains its initial parity, whereas when the axisymmetric solution is of mixed parity type, then even an eventually pure parity perturbation becomes mixed. Components Am and Sm are locked, and it is meaningless to talk of one of these modes decaying faster than the other.

4.4. *Results*

The stability of several models to $m = 1$ perturbations was investigated. (It was assumed that $m = 1$ would be the "worst" non-axisymmetric perturbation.) For the α^2-dynamo ($C_\omega = 0$) at $C_\alpha = 10$ the axisymmetric solutions display a "watershed" effect, the eventual steady solution being of S0 or A0 type, depending on

Table 4. Summary of some solutions for the $\alpha\omega$-dynamo for different C_α and $C_\omega = -10^3$. Their stability is indicated in the first column (s for stable, u for unstable). The third column, denoted by E, gives the minimum and maximum values of the total magnetic energy. The next column contains the value of P. In the case of mixed parity solutions the range covered by P is indicated. Ω_{cyc} is the magnetic cycle frequency. In the last column the type of solution is given (limit cycle or torus) and, in the case of torus solutions, the frequency ratio of short and long term oscillations is also shown. The numerical resolution is 21×41 mesh points

	C_α	E	P	Ω_{cyc}	
s	7.0	0.13...0.33	−1	56.2	l.c.
s	7.5	0.18...0.44	−1	57.0	l.c.
s	8.0	0.14...0.34	−0.39... −0.07	60.9	l.c.
s	8.5	0.17...0.62	−0.94... +0.58	59.6	torus 34
s	9.0	0.21...0.73	−0.96... +0.79	63.5	torus 30
u	10.0	0.40...0.92	−1	63.2	l.c.
s	10.0	0.71...1.58	+1	66.8	l.c.

© European Southern Observatory • Provided by the NASA Astrophysics Data System

1990A&A...230..463J

the initial conditions (see Brandenburg et al., 1989a). We find that the S0 mode is unstable against S1 perturbations ($d \ln E/dt \approx 0.64$), but stable against A1 perturbations ($d \ln E/dt \approx -2.0$). The A0 mode turns out to be stable against S1 and A1 perturbations, ($d \ln E/dt \approx -0.30$ and -3.6 respectively). These results are in agreement with those of Rädler and Wiedemann (1989) and Rädler et al. (1990).

Now we turn to the more interesting case of the $\alpha^2\omega$-dynamo. Consider first the axisymmetric torus type solution for $C_\alpha = 8.5$. As mentioned above, the A1 and S1 perturbations cannot now be separated. At all points during the long torus cycle (period ≈ 1.85) the solution is stable, with a very short decay time for the perturbations. Also for $C_\alpha = 8.0$, where the axisymmetric solution is a mixed parity limit cyle, the perturbation decays rapidly.

These results demonstrate that there is only one stable steady solution of pure parity type for the α-quenched, α^2-dynamo (since a pure nonlinear non-axisymmetric mode cannot exist), and that the unsteady mixed parity $\alpha^2\omega$-solutions are stable to small amplitude non-axisymmetric and axisymmetric perturbations. The α^2 A0 mode is, of course, unstable to large amplitude axisymmetric perturbations, which in the axisymmetric analysis take it into the S0 mode, which itself is unstable to S1 perturbations. The ultimate fate of such a system cannot be determined with the present method. However, the recent analysis of Rädler et al. (1989) shows that the solution does not settle to an unsteady mixture of axisymmetric and non-axisymmetric parts, but eventually it finds its way back to the A0 configuration. The stability of the $\alpha^2\omega$-solutions is perhaps not altogether surprising, as at $C_\omega = -10^3$ the non-axisymmetric modes are very hard to excite in a model with a prescribed, time invariant α-profile. However the possibility of a bifurcation from the mixed parity branches at lower dynamo number than that of the non-axisymmetric bifurcation from the trivial solution cannot, a priori, be discounted.

5. Conclusions

The understanding of complicated physical systems by means of truncated and simplified models is useful in order to demonstrate the different phenomena possible in more elaborate models and perhaps also in nature. We have shown that there are certain bifurcation features in simple 1-D models, which can also be found in more realistic 2-D models, for example, the transition between two states of pure parity via a mixed parity solution. However, a very detailed comparison between these approaches is not justified. On the other hand, the neglection of "curvature terms" and cutting off the polar regions from the computational domain seems to affect the solutions only slightly. This can therefore be a useful approximation in simplifying simulations of convective dynamos.

Being aware of the limitations due to models without radial extension we have demonstrated the possibility that $\alpha\omega$-dynamos can possess mixed solutions containing non-axisymmetric contributions. This result may be of relevance for understanding secular modulations of stellar light curves and probably also of the solar active longitudes. In the mean-field model non-axisymmetric magnetic fields seemed to be possible only for dynamos with weak differential rotation, because for strong differential rotation the excitation of non-axisymmetric solutions is much harder than of axisymmetric solutions. Thus an explanation of the observed non-axisymmetric contributions in solar and stellar mean fields via secondary bifurcations appears to be more likely. For example, photometric light curves of an FK Comae-type star (Jetsu et al., 1989) can be interpreted in terms of a mixed solution (quasiperiodic A0+S1). It remains to be seen if such behaviour is borne out in more detailed models with radial extension. For positive dynamo numbers the 2-D model does favour non-axisymmetric fields (S1), which is certainly an artifact of neglecting the radial extension. Therefore a full 3-D analysis is necessary in order to draw more precise conclusions. At least for only slightly supercritical dynamo numbers it seems to be reasonable to assume the solutions of $\alpha\omega$-dynamos to be axisymmetric. In particular axisymmetric mixed parity solutions with long-term variations prove to be stable against 3-D perturbations.

However, there are still many uncertainties associated with more realistic models for solar and stellar dynamos. The location and extent of the dynamo inside the star is still at present unresolved. The solar internal angular velocity has been measured in recent years with increasing success (e.g. Libbrecht, 1989; Brown and Morrow, 1987) using helioseismology as the basic tool. However the accuracy achieved is still not enough to rule out conclusively certain models, e.g. those which have $\partial\Omega/\partial r < 0$ at some depth beneath the equator.

While linear $\alpha\omega$-dynamos easily reproduce the observational requirements of migrating dynamo waves with the correct latitudinal structure, and toroidal and poloidal components with the correct phase and amplitude relations (Stix, 1976), there is still considerable uncertainty regarding nonlinear dynamos. It is generally accepted that the solar cycle is a nonlinear oscillator, partly because phenomena like the recurrence of Grand Minima (see e.g. Stuiver and Braziunas, 1988) are highly suggestive of nonlinearity. Nevertheless, our models show such nonlinear behaviour to be model dependent, sensitive to both the geometry used and the form of the nonlinearities considered. The dominating nonlinearities operating in the dynamos of various cosmical objects are still not well determined. This leaves us to make heuristic selections of nonlinear terms which are related to properties of the full equations. It is reasonable to consider α-quenching when treating mean fields, but our results show that if the solar dynamo really does work in a thin layer beneath the convection zone then such α-quenching leads to the "wrong" type of nonlinear behaviour, that is only a steady quadrupolar solution exists, even for a wide range of dynamo numbers. The other nonlinearity considered here – buoyancy – is motivated by the observations of sunspots and theory (Parker, 1955; Spiegel and Weiss, 1982).

Magnetic activity cycles for other stars are now well established (see e.g. Soderblom and Baliunas, 1988), and show the Sun not to be a special case. It is found that stars with similar age, mass, and rotation rate as the Sun can have a range of behaviour, including virtually steady activity. While it is tempting to link such observations to the rich and varied responses of our theoretical models, we do not feel that this is yet justified. Instead we conclude that there is still a great deal to be learnt about nonlinear stellar cycles, and that progress may be made by careful studies which simultaneously use "exploratory" idealised systems together with more sophisticated models.

Acknowledgements. This work developed from a spell of collaboration at the University of Helsinki. R. Jennings and D. Moss wish to thank the Helsinki group for initiating their visits. R. Jennings is also indebted to S.E.R.C. and the University of Helsinki for financial support.

© European Southern Observatory • Provided by the NASA Astrophysics Data System

1990A&A...230..463J

References

Bai, T.: 1988, *Astrophys. J.* **328**, 860

Brandenburg, A., Krause, F., Meinel, R., Moss, D., Tuominen, I.: 1989a, *Astron. Astrophys.* **213**, 411

Brandenburg, A., Moss, D., Tuominen, I.: 1989b, *Geophys. Astrophys. Fluid Dyn.* **49**, 129

Brandenburg, A., Meinel, R., Moss, D., Tuominen, I.: 1990, in *Solar Photosphere*, ed. J.O. Stenflo, Reidel, Dordrecht, p. 379

Brown, T.M., Morrow, C.A.: 1987, *Astrophys. J. Letters* **314**, L21

Gilman, P.A., Miller, J.: 1981, *Astrophys. J. Suppl.* **46**, 211

Greenspan, H.P.: 1974, *Stud. Appl. Math.* **34**, 35

Howard, R., LaBonte, B.J.: 1980, *Astrophys. J. Letters* **239**, L33

Hughes, D.W.: 1985, *Geophys. Astrophys. Fluid Dyn.* **32**, 273

Jennings, R., Weiss, N.O.: 1990a, in *Solar Photosphere*, ed. J.O. Stenflo, Reidel, Dordrecht, p. 355

Jennings, R., Weiss, N.O.: 1990b, *Monthly Notices Roy. Astron. Soc.* (submitted)

Jetsu, L., Huovelin, J., Tuominen, I., Vilhu, O., Bopp, B.W., Piirola, V.: 1989, *Astron. Astrophys.* (submitted)

Köhler, H.: 1973, *Astron. Astrophys.* **25**, 467

Krause, F., Meinel, R.: 1988, *Geophys. Astrophys. Fluid Dyn.* **43**, 95

Libbrecht, K.G.: 1989, *Astrophys. J.* **336**, 1092

Lorenz, E.N.: 1963, *J. Atmosph. Sci.* **20**, 130; **20**, 448

Moss, D., Tuominen, I., Brandenburg, A.: 1990, *Astron. Astrophys.* (in press)

Parker, E.N.: 1955, *Astrophys. J.* **121**, 491

Parker, E.N.: 1979, *Cosmical Magnetic Fields*, Clarendon Press, Oxford

Piskunov, N.E., Tuominen, I., Vilhu, O.: 1990, *Astron. Astrophys.* (in press)

Rädler, K.-H.: 1986a, *Astron. Nachr.* **307**, 89

Rädler, K.-H.: 1986b, *Plasma Physics*, ESA SP-251, 569

Rädler, K.-H., Wiedemann, E.: 1989, *Geophys. Astrophys. Fluid Dyn.* **49**, 71

Rädler, K.-H., Wiedemann, E., Brandenburg, A., Meinel, R., Tuominen, I.: 1989, *Astron. Astrophys.* (submitted)

Schüssler, M.: 1983, in *Solar and stellar magnetic fields*, ed. J.O. Stenflo, Reidel, Dordrecht, p. 213

Soderblom, D.R., Baliunas, S.L.: 1988, in *Secular Solar and Geomagnetic Variations over the last 10,000 Years*, eds. F.R. Stephenson, A.W. Wolfendale, Kluwer, Dordrecht, p. 25

Spiegel, E.A., Weiss, N.O.: 1982, *Geophys. Astrophys. Fluid Dyn.* **22**, 219

Steenbeck, M., Krause, F.: 1969, *Astron. Nachr.* **291**, 49

Stix, M.: 1971, *Astron. Astrophys.* **13**, 203

Stix, M.: 1975, *Astron. Astrophys.* **42**, 85

Stix, M.: 1976, in *Basic Mechanisms of Solar Activity*, eds. V. Bumba, J. Kleczek, Reidel, Dordrecht, p. 367

Stuiver, M., Braziunas, T.F.: 1988, in *Secular Solar and Geomagnetic Variations over the last 10,000 Years*, eds. F.R. Stephenson, A.W. Wolfendale, Kluwer, Dordrecht, p. 245

Weiss, N.O., Cattaneo, F., Jones, C.A.: 1984, *Geophys. Astrophys. Fluid Dyn.* **30**, 305

© European Southern Observatory • Provided by the NASA Astrophysics Data System